Vibrational spectroscopy of $GdCr_3(BO_3)_4$: quantitative separation of crystalline phases

E A Dobretsova[1], K N Boldyrev[1], M N Popova[1], V A Chernyshev[2], E Yu Borovikova[3], V V Maltsev[3] and N I Leonyuk[3]

[1]Institute for Spectroscopy Russian Academy of Sciences, Moscow, Troitsk, 108480, Russia
[2]Ural Federal University, Ekaterinburg, 620002, Russia
[3]Department of Crystallography and Crystal Chemistry, Faculty of Geology, Moscow State University, Moscow, 119991, Russia.

E-mail: elena-dobrecova@yandex.ru

Abstract. This work is devoted to the investigation of $GdCr_3(BO_3)_4$ crystals by the method of infrared spectroscopy. Incongruently melting borate $GdCr_3(BO_3)_4$ was obtained as a result of spontaneous crystallization. Crystal structures were identified by the method of infrared spectroscopy. *Ab initio* calculations in the frame of density functional theory enabled us to separate modes belonging to the *R*32 and *C*2/*c* phases and to estimate the ratio of these phases in $GdCr_3(BO_3)_4$ crystals. We have found that the content of the rhombohedral *R*32 (non-centrosymmetric) modification is about 85 %.

1. Introduction

Rare-earth (RE) borates described by the general formula $RM_3(BO_3)_4$ (*R* = RE or yttrium, *M* = Al, Ga, Sc ,Fe, or Cr) crystallize in a number of space groups (SG) with structure type of the natural mineral huntite [1]. These compounds are of interest due to their optical, magnetic, and magnetoelectric properties [2, 3]. RE aluminum borates possess excellent luminescent, nonlinear optical, thermal, and mechanical properties, are chemically stable and are widely used in self-frequency doubling and self-frequency summing lasers [4-6]. RE iron [7-11], aluminum [12-15] and gallium [16] borates demonstrate attractive magnetoelectric properties. Materials with a large magnetoelectric effect have an application potential as magnetoelectric sensors, magneto-electric and electro-magnetic memory elements, etc. It is important to notice that nonlinear optical and magnetoelectric properties are characteristic only for non-centrosymmetric structures.

RE chromium borates have polytype nature and crystalize in two modifications, namely, the rhombohedral one with the non-centrosymmetric SG *R*32 or the monoclinic one with the centrosymmetric SG *C*2/*c*. The crystal type depends on the growth conditions. Moreover, a coexistence of differently ordered structural fragments in one single crystal is a characteristic feature of RE chromium borates. [17, 18].

The objective of our present study are to identify the crystal structure of $GdCr_3(BO_3)_4$ obtained by the method of spontaneous crystallization and to evaluate its potential for practical applications.

2. Crystal structure of huntite-like borates

As was already mentioned in Introduction, RE borates have the structure type of huntite $CaMg_3(CO_3)_4$. The latter one crystallizes in the SG *R*32 [19]. Three types of coordination polyhedra are present in this structure, namely, CaO_6 trigonal prisms, MgO_6 octahedra and two types of CO_3 plain triangles [20] The MgO_6 octahedra are connected by common edges forming chains along the *c* axis. The RO_6 trigonal prisms are isolated from each other. In the rare-earth double borates, Ca atoms are replaced by RE elements but instead of Mg atoms one finds *M* cations (which form a quasi-one-dimensional magnetic system in the case of Fe^{3+} and Cr^{3+} ions) [21]. The CO_3^{2-} groups are replaced by the BO_3^{3-} triangles (figure 1).

Besides the rhombohedral *R*32 structure there is a monoclinic one with SG *C*2/*c*. In each of these two structures it is possible to distinguish two different types of layers, L_{2n} and L_{2n+1}, identical for two modifications (figure 2). The first type layer (L_{2n}) contains pairs of edge-sharing MO_6 octahedra which are further connected into a layer via isolated BO_3 triangles. The second one (L_{2n+1}) is built by trigonal RO_6 prisms and MO_6 octahedra connected in columns by vertices and also connected via the BO_3 triangles. In the rhombohedral (SG *R*32) polytype, the L_{2n+1} layers which contain prisms are multiplied around the L_{2n} layers by two-fold axes, whereas in the monoclinic modification (SG *C*2/*c*) by centers of symmetry [22, 23].

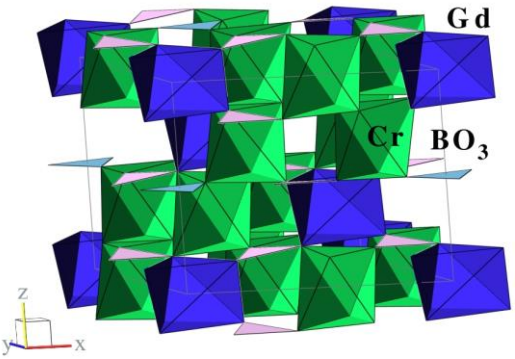

Figure 1. Crystal structure of $GdCr_3(BO_3)_4$ with SG *R*32

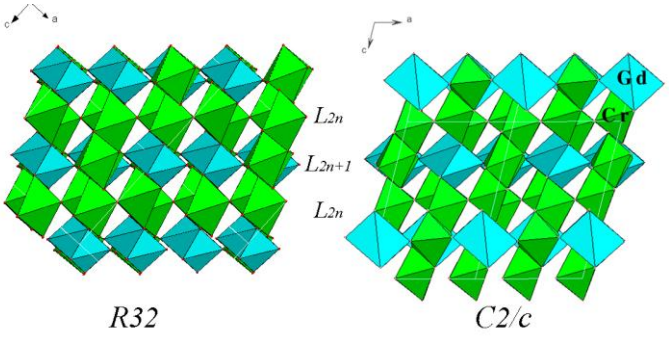

Figure 2. Schematic structures of $GdCr_3(BO_3)_4$ with: a) SG *R*32 (D_3^7) and b) SG *C*2/*c* (C_{2h}^6)

3. Experimental and computational details

3.1. Sample preparation

The incongruently melting borate $GdCr_3(BO_3)_4$ was obtained from a molten solution on the basis of K_2MoO_4 - $3MoO_3$ as a result of spontaneous crystallization. Experiments were conducted with a ratio of the borate to the solvent in the mixture 1:1. The crucible with the charge was maintained in a furnace until a complete homogenization of the melt for 5 hours at 1100 – 1150 °C. Thereafter, the temperature was lowered to 1000 °C at a rate of 2 °C/h, then at a rate of 1°C/h to 840 °C and to 300 °C at a rate of 10 °C/h. Crystallization of the borate occurred at 1050 - 840˚C.

For infrared measurements, a single crystal was grinded into a powder in a pobedite mortar.

3.2. Measurements by the methods of infrared spectroscopy

Absorption spectra of the powder sample of $GdCr_3(BO_3)_4$ in the far-infrared (FIR) region 50–550 cm^{-1} were registered with the help of a Bruker IFS 125HR Fourier spectrometer (the spectral resolution was up to 2 cm^{-1}), using polyethylene disc technique. The infrared absorption spectra in the middle IR region (MIR) 550-1600 cm^{-1} were registered on the same spectrometer with an attenuated total reflection (ATR) module. The powder sample was pressed to a diamond crystal of the ATR module. The spectral resolution was 2 cm^{-1}. We applied methods of vibrational spectroscopy combined with the group-theoretical analysis [24] in order to understand the peculiarities of the structure of the $GdCr_3(BO_3)_4$ borate.

3.3. Ab initio calculations

Ab initio calculations of phonon frequencies and intensities of the infrared-active modes in $GdCr_3(BO_3)_4$ were performed for both *R32* and *C2/c* structures in a frame of the density functional theory (DFT) with hybrid functional B3LYP. The calculations were carried out within MO LCAO approach implemented in CRYSTAL14 code. Non-relativistic pseudopotential was used to describe the inner shells of the rare-earth ion. Details of the calculations can be found in Ref. [25].

4. Results of IR measurements and DFT calculations

Figure 3 shows the IR spectrum in the region 50-1600 cm^{-1}. It is typical for RE chromium borates with the SG *R*32. The majority of the observed modes find their counterparts in the calculated energy spectrum for this phase of $GdCr_3(BO_3)_4$. It is not possible to extract oscillator strengths from the measured spectra of powder samples. But we have to note that, in general, large calculated oscillator strengths correspond to strong lines in the measured spectrum, whereas for low ones one finds either weak lines or no line at all (see Table 1). Thus, the calculated data for the *R*32 phase are in good agreement with the experimental ones, which, in turn, confirms the assumption of predominantly rhombohedral structure of gadolinium chromium borate.

However, several features point to the presence of a monoclinic phase fragment. For internal vibrations of BO_3^{3-} groups, they are (i) a shoulder at 747 cm^{-1} in the region of the symmetric bending vibrations, (ii) a splitting of the band at 980 cm^{-1} in the region of the symmetric stretching vibrations, and (iii) shoulders at 1278 and 1372 cm^{-1} in the region of asymmetric stretching vibrations (Figure 3, Table 1). In the FIR region, translational vibrations of the Gd^{3+} and Cr^{3+} ions, as well as translational and librational motions of the BO_3^{3-} groups are observed. Signatures of monoclinic inclusions in this spectral region are (i) a weak band at 73 cm^{-1} of the Gd^{3+} vibrations, (ii) bands at 126, 148, and 275 cm^{-1}, (iii) a weak shoulder at 248 cm^{-1} due to the BO_3^{3-} vibrations, and (iv) a splitting of the band at 434 cm^{-1} in the region of Cr^{3+} vibrations. (Figures 3 and 4, Table 1).

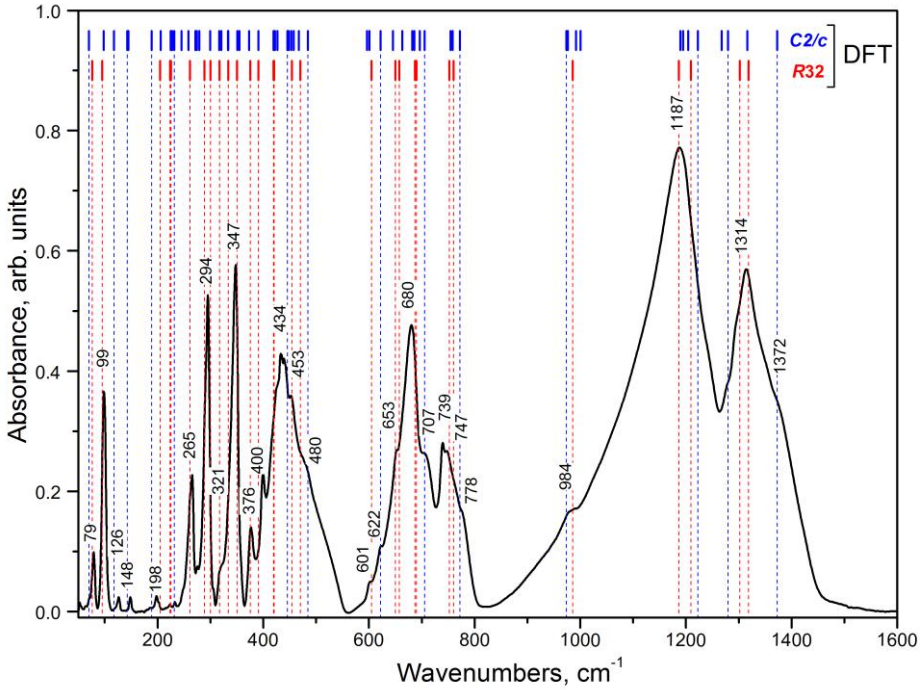

Figure 3. Infrared spectrum of $GdCr_3(BO_3)_4$. At the upper part of the figure, results of the *ab initio* calculations for the *R*32 (red bars) and *C*2/*c* (blue bars) phases are presented.

Table 1. Comparison between calculated and experimentally observed vibrational modes of $GdCr_3(BO_3)_4$ in the *R*32 phase. The assignments of particular modes are also given in accordance with the calculated eigenvectors. Experimental extra peaks ascribed to the monoclinic C2/*c* phase are in bold (their symmetry is indicated in parentheses). The corresponding calculated frequencies are plotted in Figures 3 and 4.

Assignments		*Ab initio* calculations		Experiment
		Wavenumbers, cm^{-1}	Oscillator strength	Wavenumbers, cm^{-1}
A_1	L BO_3^{3-}	216		
	T (BO_3^{3-}) T (Gr^{3+})	342		
		495		
	ν_4	660		
	ν_1	975		
		1004		
	ν_3	1209		
A_2	T (Gd^{3+})	76	2,97	**73 sh (B_u)** 79 m
	L (BO_3^{3-})	205	0,11	**126 w (B_u)** **148 w (B_u)** 198 w
		225	0,001	233 w
		261	0,72	265 s **275 w (A_u)**
	T (BO_3^{3-}) T (Cr^{3+})	289	0,17	290 sh
		334	0,78	321 w
		391	0,32	400 s
		419	0,91	424 sh
	ν_4	657	0,0004	653 sh
	ν_2	690	0,73	707 sh
		760	0,12	778 sh
	ν_3	1302	0,02	**1278 sh (B_u)** 1296 sh
E	T (R^{3+})	95	2,08	99 s
	L (BO_3^{3-})	205	0,0005	202 w sh
		224	0,0016	223 w
		261	0,044	**248 sh (Bu)** 262 sh
		300	0,36	294 s
	T (BO_3^{3-}) T (Cr^{3+})	317	0,05	306 w
		351	0,15	347 s
		375	0,015	376 m
		420	0,33	434 s **440 s (Bu)**
		454	1,80	453 m
		470	0,00007	480 sh
	ν_4	605	0,0011	601 w
		650	0,0038	622 w
		687	0,053	680 s
	ν_2	752	0,017	739 s **747 sh (Au)**
	ν_1	986	0,005	980 w **990 w (Bu)**
	ν_3	1187	0,78	1187 s
		1210	0,001	-
		1318	0,30	1314 s **1372 sh (Au)**

sh – shoulder, w – weak, s – strong, m – medium

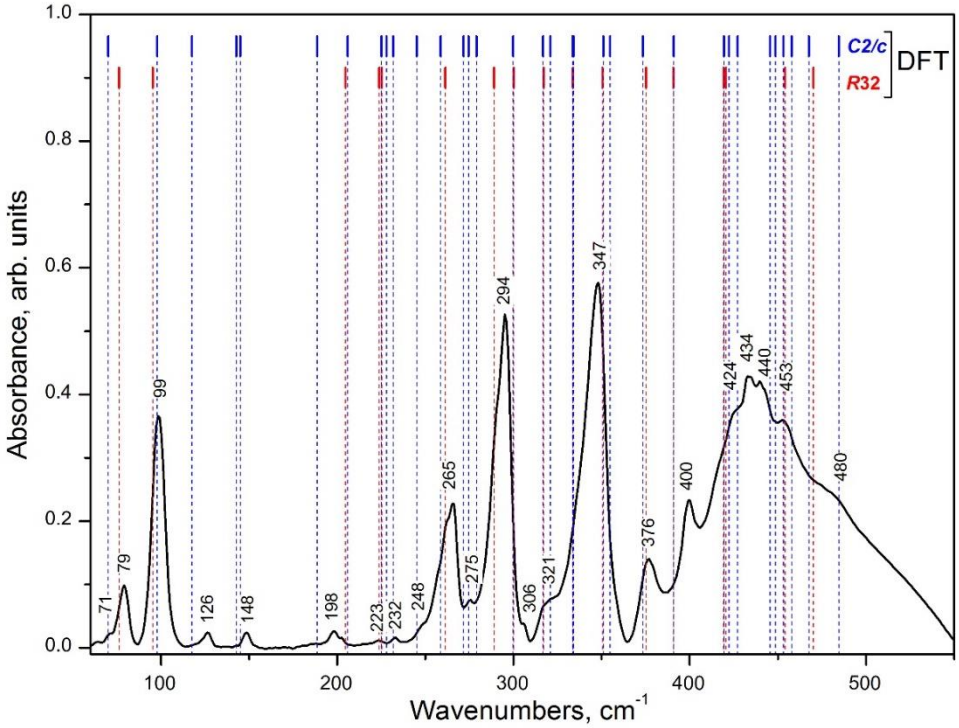

Figure 4. FIR part of the spectrum of $GdCr_3(BO_3)_4$.

5. Estimate of the relative quantity of the monoclinic phase in the sample

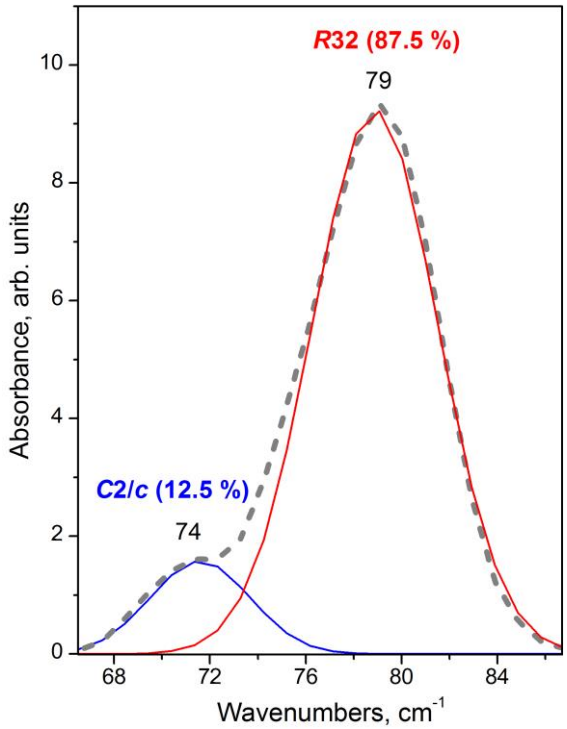

Figure 5. Long-wavelength part of the absorption spectrum of $GdCr_3(BO_3)_4$ (dashed grey line). Decomposition into two Gaussian peaks is shown by thin lines.

Figure 5 shows the experimental IR spectrum at long wavelengths where the translational vibrations of Gd^{3+} are observed. The band at 79 cm^{-1} has a shoulder 73 cm^{-1}, which is associated with a small admixture of the monoclinic phase. We have fitted the experimental spectrum by two Gaussians and found that the intensity of the strongest band constitutes 82.3%. According to calculations, the oscillator strength of the considered vibration in the monoclinic phase is 1.5 times greater than in the rhombohedral one. Taking into account this value, we could estimate that the content of the rhombohedral phase in the sample was about 87.5%.

6. Conclusions

Good quality single crystals of gadolinium chromium borate with the structure of the mineral huntite were obtained by spontaneous crystallization from the flux. IR spectroscopy delivered experimental data on the IR-active phonons. The data were compared with the results of *ab initio* DFT calculations. This comparison shows that the crystal has a polytype structure, containing mainly the rhombohedral phase *R32* and a small part of the monoclinic phase *C2/c*. The *ab initio* calculations allowed us to distinguish between vibrations belonging to the one and the other structural phases. From the relative intensities of the two low-frequency bands corresponding to translational motions of Gd in the *R32* and *C2/c* phases and taking into account the calculated oscillator strengths, we were able to evaluate the content of monoclinic phase in the predominantly rhombohedral single crystal of $GdCr_3(BO_3)_4$, which was around 15%. Thus, we have shown that the gadolinium chromium borate crystallizes, mainly, in the noncentrosymmetric phase *R*32. This indicates a potential of owning magnetoelectric properties, by analogy with noncentrosymmetric iron, aluminium and gallium RE borates. Currently, the work is underway to obtain large single-phase crystals of $GdCr_3(BO_3)_4$ for investigation of the magnetoelectric effect.

Acknowledments

This work was supported by the Russian Science Foundation under Grant No 14-12-01033 and by the President of Russian Federation (D.E.A. project СП-754.2015.1).

References

[1] Leonyuk N I and Leonyuk L I 1995 *Prog. Cryst. Growth and Charact.* **31** 179
[2] Dorozhkin L M, Kuratev I I, Leonyuk N I, Timchenko T I and Shestakov A V 1981 *Sov. Tech. Phys. Lett.* **7 (11)** 555
[3] Leonyuk N I, Maltsev V V, Volkova E A, Koporulina E V, Nekrasova N V, Tolstik N A and Kuleshov N V 2009 *J. Physics: Conf. Series* **176** 012010A
[4] Nikogosyan D N 2005 *Nonlinear Optical Crystals: A Complete Survey* Springer Berlin
[5] Brenier A, Tu C, Zhu Z and Wu B 2004 *Appl. Phys. Lett.* **84** 2034
[6] Jaque, D. J. 2001 *Alloys and Comp*. **323–324** 204
[7] Mukhin A A, Vorob'ev G P, Ivanov V Yu, Kadomtseva A M, Narizhnaya A S, Kuzmenko A M, Popov Yu F, Bezmaternykh L N and Gudim I A 2011 *JETP Lett.* **93(5)** 275
[8] Zvezdin A K, Krotov S S, Kadomtseva A M, Vorob'ev G P, Popov Yu F, Pyatakov A P, Bezmaternykh L N and Popova E A 2005 *JETP Lett.* **81(6)** 272
[9] Kadomtseva A M, Popov Yu F, G. P. Vorob'ev, Pyatakov A P, Krotov S S, Kamilov K I, Ivanov V Yu, Mukhin A A, Zvezdin A K, Kuz'menko A M, Bezmaternykh L N, Gudim I A and Temerov V L 2010 *Low Temp. Phys.* **36(6)** 511
[10] Zvezdin A K, Vorob'ov G P, Kadomtseva A M, Popov Yu F, Pyatakov A P, Bezmaternykh L N, Kuvardin A V and Popova E A 2006 *JETP Lett.* **83(11)** 509
[11] Popov Yu F, Pyatakov A P, Kadomtseva A M, Vorob'ov G P, Zvezdin A K, Mukhin A A and Ivanov V Yu 2010 *JETP* **138(2)** 226
[12] Liang K - C, Chaudhury R P , Lorenz B, Sun Y Y, Bezmaternykh L N, Temerov V L and Chu C W 2011 *Phys. Rev. B* **83** 180417
[13] Begunov A I, Demidov A A, Gudim I A and Eremin E V 2013 *JETP Lett.* **97(9)** 528

[14] Kadomtseva A M, Popov Yu F, Vorob'ev G P, Kostyuchenko N V, Popov A I, Mukhin A A, Ivanov V Yu, Bezmaternykh L N, Gudim I A, Temerov V L, Pyatakov A P and Zvezdin A K 2014 *Phys. Rev. B* **89(1)** 014418
[15] Chaudhury R P, Lorenz B, Sun Y Y, Bezmaternykh L N, Temerov V L and Chu C W 2010 *Phys. Rev. B* **81(22)** 220402
[16] Volkov N V, Gudim I A, Eremin E V, Begunov A I, Demidov A A and Boldyrev K N 2014 *JETP Lett.* **99(2)** 67
[17] Borovikova E Yu, Dobretsova E A, Boldyrev K N, Kurazhkovskaya V S, Maltsev V V and Leonyuk N I 2013 *Vibr. spectrosc*. **68** 82
[18] Kurazhkovskaya V S, Dobretsova E A, Borovikova E Yu, Mal'tsev V V and Leonyuk N I, 201 *J. Struct. Chem.* **52**(4) 699
[19] Mills A D 1962 *Inorg. Chem.* **1**(4) 960
[20] Dollase W A and Reeder R J 1986 *Amer. Miner.* **71(1-2)** 163
[21] Campá J A, Cascales C, Gutiérrez-Puebla E,Monge M A, Rasines I and Ruíz-Valero C 1997 *Chem. Mater.* **9**(1) 237-240.
[22] Belokoneva E L and Timchenko T I 1983 *Sov. Phys. Crystallogr.* **28** 658
[23] Plachinda P A and Belokoneva E L 2008 *Cryst. Res. Technol.* **43** 157
[24] Fausti D, Nugroho A A, van Loosdrecht P H M, Klimin S A, Popova M N, Bezmaternykh L N 2006 *Phys. Rev. B* **74** 024403
[25] Chernyshev V A, Nikiforov A E, Petrov V P, Serdtsev A V, Kaschenko M A and Klimin S. 2016 *Phys. Sol. St.* **58 (8)** 1587